Chiang Mai J. Sci. 2018; 45(6) : 2361-2373
http://epg.science.cmu.ac.th/ejournal/
Contributed Paper

Modification of Anti-cancer Co-crystal for Thymidylate Synthase Inhibition: Molecular Dynamics Study

Nadia Hanim Sabri [a], Siti Nadiah Abd. Halim [b], Sharifuddin Md Zain [a] and Vannajan Sanghiran Lee* [a]

[a] Department of Chemistry, Center of Theoretical and Computational Physics (CTP, Faculty of Science, University of Malaya, Kuala Lumpur 50603, Malaysia.

[b] Department of Chemistry, Faculty of Science, University of Malaya, Kuala Lumpur 50603, Malaysia.

* Author for correspondence; e-mail: vannajan@gmail.com

Received: 1 December 2017
Accepted: 24 January 2018

ABSTRACT

Raltitrexed (tomudex) is an alternative antifolate drug to 5-fluorouracil (5-FU) to inhibit thymidylate synthase (TS) by decreasing dihydrofolate reductase (DHFR) activity. The clinical trial shows the potential of raltitrexed towards TS inhibition can be enhanced by combining the raltiterexed with other anticancer agents. This present work discovered the combination of raltitrexed with modifying 5-FU based co-crystal (compound 1) have high effectiveness with manageable toxicity via computational approach. The X-ray structure of human TS (1HVY) was retrieved from Protein Database Bank. The molecular docking of protein-ligand complexes has been performed to investigate the potential of ligands as TS inhibitor by disrupting both promising binding sites; nucleotide and folate. The best-ranked conformations were further explored via parameterized molecular dynamic simulation. The simulated result by molecular dynamic simulation suggested that the modified co-crystal (compound 1) enhancing binding strength of raltitrexed to inhibit TS with binding free energy (-45.68 kcal/mol) compared to raltitrexed alone (-16.57 kcal/mol). Per-residue decomposition revealed that the Arg50A, Leu192A, Cys195A, His196A, Asn226 and Gly217A are the pivotal residues that playing main role in the nucleotide binding site. The binding free energy in the folate binding site is majority come from the interaction with Phe80A, Ile108A, Trp109A, Asp218A, Phe225A, Tyr258A, Met311A and Ala312A residues.

Keywords: colorectal cancer, raltitrexed, 5-fluorouracil (5-FU), compound 1, thymidylate synthase (TS), molecular dynamic simulation, MM-PBSA/GBSA

1. INTRODUCTION

Thymidylate synthase (TS) is an essential precursor for DNA that has significant point in cancer chemotherapy since its overexpression in numerous cancer types show oncogene like activity and reduce the translational efficiency of mRNA [1]. Thus, thymidylate destruction can be achieved by reduction of TS catalytic activity leading to cell death [2]. Nucleotide (dUMP) and folate (5,10-CH_2 THF) are promising binding sites

for TS disruption [3].

Raltitrexed (tomudex) is an analogue of the 5,10-CH_2THF cofactor that inhibits TS specifically by targeting folate binding site through rapid polyglutamation by enzyme FPGS and transported into cells through the folate transporter (FOLT) [4]. 5-fluorouracil (5-FU) is a fluoropyrimidine-based drug that works through nucleotide binding site, then blocking the RNA synthesis and incorporation into DNA leading to DNA strand breaks [5]. Nevertheless, the incorporation action contributes to 5-FU cytotoxicity and monotherapy of 5-FU gives an ineffective result due to drug resistance. The combination of raltitrexed with antitumor drugs from different mechanism action offer improvement in effectiveness whilst retaining the manageable toxicity profile. A summary of phase I and II trial indicate that the combination of raltitrexed with 5-FU gave a promising result with manageable tolerability and favourable response rates [6].

In previous work, a series of 5-Fluorouracil (5-FU) co-crystals derivatives were synthesized and the potential anti-cancer activity without raltitrexed has been explored by molecular docking study [7]. The co-crystals were structurally formed by cocrystallization of 5-FU as API and a series of conformer in definite stoichiometric amounts. The target protein (TS) - ligand complexes model were generated using molecular modelling approach to rationalize the activity of co-crystal and to predict the most favourable interaction. It revealed that 5-FU based co-crystals has potential as an anti-cancer with strong binding interaction.

Here, the modification of selected co-crystal (compound 1) has been performed to intensify the binding affinity and stability by fragment linking approach. The potential of compound 1 to enhance the effectiveness of raltitrexed for TS inhibition was evaluated via molecular docking with 1HVY, X-ray structure of human TS complex in the present of raltitrexed. The idea of this combination is logical since they have the different mechanism of actions. Both possible binding sites were disrupted where compound 1 targeting nucleotide binding site whilst raltitrexed for folate binding site. We were exploring the theoretical modelling and molecular dynamics simulation of co-crystals and compound 1 with raltitrexed against TS to analyse the stability of the complexes. For validating the protein-ligand interaction, we were further analysed relative binding free energy prediction by using molecular mechanics/Poisson-Boltzmann surface area (MM-PBSA) and molecular mechanics/generalized born surface area (MM-GBSA) method.

2. MATERIALS AND METHODS

2.1 Modification of Co-crystal

The co-crystal (5FU-U) was modified by fragment linking approach to enhance the stability and binding interaction (figure 1). Compound 1 was structurally connected through heptyl group to mimic the reference ligand (dUMP). It was optimized by employing DFT method with B3LYP/6-311G** in Gaussian09 program (Gaussian, Inc) [8, 9]. The optimized geometry was further used for docking study.

2.2 ADMET Prediction

The computer aided for absorption, distribution, metabolism, elimination, and toxicity (ADMET) prediction was evaluated by using ADMET descriptors in Discovery Studio 2.5 [10]. The ADMET absorption parameter predicts the human intestines absorption (HIA) after oral administration and the solubility of compounds are predicted by ADMET aqueous solubility

due to the genetic partial square method with experimentally measured solubility [11]. The blood-brain penetration of molecule after oral administration is predicted through ADMET blood-brain barrier (BBB) parameter. The binding levels prediction were based on the marker similarities due to the conditions on calculated log P [12]. The probability of compound to be cytochrome P450 2D6 enzyme inhibitor has been predicted via ADMET CYP2D6 binding [13]. ADMET hepatotoxicity predicts the hepatotoxic nature of the compound based on the known compounds that exhibit liver toxicity [11].

Figure 1. The structures of (A) 5FU-U co-crystal and (B) compound 1.

2.3 Molecular Docking Study

The pdb file of the thymidylate synthase (PDB ID: 1HVY), X-ray structure of human TS-ligand-cofactor complex (chain A and chain B) deposited in RCSB protein data bank (http://www.pdb.org) has been used. 1HVY is the closed conformation of recombinant hTS complex with dUMP and raltitrexed (Tomudex, ZD1694), as an antifolate drug at 1.9Å resolution [14]. The docking procedure of dUMP, 5FU-U co-crystal and compound 1 with raltitrexed were conducted by using CDOCKER protocol in the receptor-ligand interaction of Discovery Studio Client 2.5 [10]. CDOCKER is a molecular docking method that employs CHARMm. All complexes were pre-treated and minimized by applying Memony Rone partial charged [15]. All ionisable residues were set at their default protonation state at a neutral pH.

CDOCKER is a rigid-flexible docking which allow ligand to flex whilst the receptor is held rigid during the refinement. The random orientations of the conformation were generated to simulated annealing molecular dynamics involving the heating up to high temperature of 700 K in 2000 steps and cooling down to 300K in 5000 steps. Since the ligands are fluoropyrimidine-based TS inhibitor, a binding location of dUMP ligand in nucleotide binding site of chain A (residue 181-197) has been selected as a target site sphere with 25Å radius [14]. The best complex structure was selected based on the CDOCKER interaction energy.

2.4 Molecular Dynamics Study

The X-ray structure of dUMP-raltitrexed complex, docking structure 5FU-U co-crystal-raltitrexed complex and docked compound 1 - raltitrexed complex have been further explored for molecular dynamic study. Deriving atomic charges of dUMP, raltitrexed and compound 1 were performed by R.E.D Tools (RESP and ESP charge derive, http://q4md-forcefieldtools.org/RED/) [16]. RESP program has been used to perform charge fitting that suitable for molecular dynamics simulation by employing different quantum mechanical. Charge values are reproduced by defining tight optimization criteria. For the preparation of ligands, the general AMBER force field (GAFF) was applied by using antechamber module [17].

Molecular dynamics (MD) simulation at the molecular mechanics level was employed using ff12SB [18] force field as implemented in AMBER12 [19] suite of programs to describe the molecular characteristics of a complex. PROPKA program has been used to assign the ionization state of an amino acid with electrical charged side chain [20]. The complexes were solvated in a cubic box of TIP3PBOX [21] water extending at 12Å in each direction from the solute with Na+ ions added as neutralizing counterions. To compute the non-bonded interactions, the cut off distance was kept to 10Å.

All simulations were performed under periodic boundary conditions and long-range electrostatic were treated by applying particle-mesh-Ewald method [22]. Energy minimization and molecular dynamics (MD) simulations were performed by using PMEMD.CUDA [23] from AMBER12 on graphical processors (GPUs) Quadro 2000D produced by NVIDIA which accelerate simulation wall time required to obtain trajectory file for each simulation. The temperature of each system was rise constantly from 0 to 310 K within 60 ps of NVT dynamics. This was proceeded with 300 ps of NPT equilibration at 310.15 K and 1 atm pressure. 75ns of NPT-MD simulation with 2fs time step was executed for properties collection.

The structural properties and intermolecular interaction of protein-ligand complexes were analysed within 75 ns of MD trajectories to identify their stability for long run simulation by using PTRAJ module of the amber package. The system stability has been verified by root mean square deviation (RMSD).

2.5 Binding Free Energy Calculation and Per-residue Free Energy Decomposition

The calculation and decomposition of binding free energy of the complexes were evaluated based on the Molecular Mechanics/Poisson-Boltzmann Surface Area (MM/PBSA) and Molecular Mechanics/Generalized Born Surface Area (MM/GBSA) protocol that implemented in AMBER12 to estimate the binding affinity between target protein (TS) and ligands [24].

Five hundred MD snapshot were extracted from the last 5ns trajectories simulation and were used as structural ensemble to evaluate the MM-PBSA/GBSA binding free energies. They were computed by Amber SANDER module [24]. Further, the per-residue free energy decomposition was carried out to obtain free energy that contributes to specific binding. This approach calculates the energy contribution of single residues by summing its interaction with all residues in the system, which are possible for molecular mechanics and free energy solvation [25].

2.6 Insight into Protein-ligand Interaction

The interaction of protein-ligand complex at 75ns was determined by Protein-Ligand Interaction Profiler (PLIP) server (https://projects.biotec.tu-dresden.de/plip-web), a novel web that serves visualization of non-covalent protein-ligands contacts in 3D [26]. The high-resolution images were generated by PyMOL 1.6 [27].

3. RESULT AND DISCUSSION

3.1 ADMET Prediction

ADMET is widely used as a first step to predict pharmacokinetics properties of drug candidates that would be toxic or not permeable to cross membranes. The result was analysed and reported as table. Since all ligands have been predicted to have low value for BBB penetration levels, they may not be able to penetrate the blood-brain barrier and

reduce the percentage of CNS side effects. In fact, compound 1 has improved the ability to absorb well through human intestinal with lower ADMET absorption level rather than 5-FU and raltitrexed.

In term of solubility, they are predicted to have high dissolution rate with optimal aqueous solubility level. Further analysis with hepatotoxicity, we found that compound 1 is expected to have less toxicity profile compared to raltitrexed and 5-FU based on low hepatotoxicity probability. In addition, all ligands have satisfied CYP2D6 result suggesting that they are non-inhibitors of CYP2D6. So, the liver dysfunction side effect is not expected upon administration of these compounds and indicates that they are well metabolized [28].Overall, compound 1 shows the potential as a drug candidate with the best pharmacokinetic properties.

3.2 The Potential of TS Inhibition

The potential of ligands to inhibit TS were analysed by molecular docking study. The overall docking structures and superimpositions of ligands for raltitrexed-dUMP complex, raltitrexed-5FU-U co-crystal complex and raltitrexed-compound 1 complex were depicted as figure S1. Based on the result, 5FU-U co-crystal and compound 1 possess a similar position with reference ligand, dUMP.

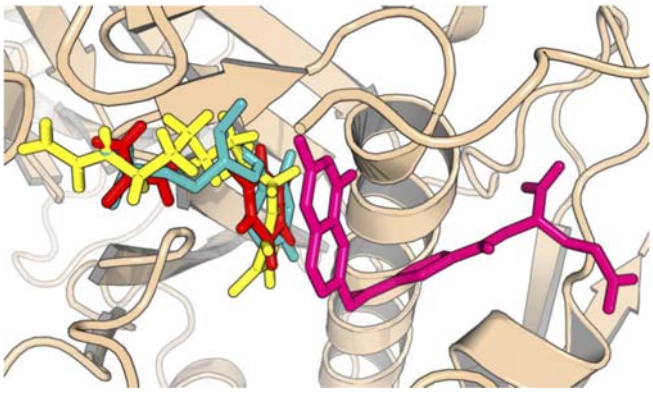

Figure S1. The overview of superimposed ligands, dUMP (blue), 5FU-U co-crystal (red) and compound 1 (yellow) with raltitrexed (pink) in a docked complex.

The strength of the protein-ligand interactions was evaluated based on CDOCKER interaction. The more negative value for CDOCKER interaction reveals strong binding between target protein (TS) and ligand. The results of docking for all ligands with TS were summarized in figure S2. As stated on the graph, 5FU-U co-crystal cannot enhance the binding affinity of raltitrexed with high interaction energy (-34.2 kcal/mol). In contrast, compound 1 in the present of raltitrexed has similar interaction energy (-45.15 kcal/mol) with raltitrexed-dUMP complex (-45.88 kcal/mol), thus express its potential to bind well with TS.

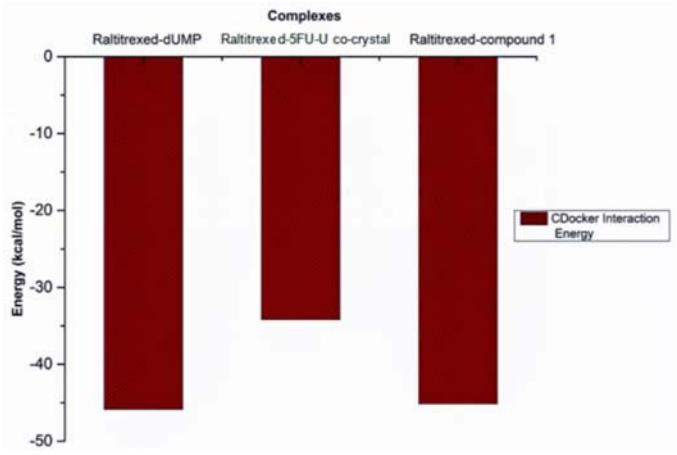

Figure S2. The docking's result of the protein-ligand complexes due to the CDOCKER interaction energy (kcal/mol).

3.3 The Stability and Flexibility of Protein-ligand Complexes

The stability of the docking complexes was assessed by probing the stability via molecular dynamic simulation. The structural properties and dynamic conformational changes of all complexes were examined by Root Mean Square Deviation (RMSD) of all C_α atoms (figure 2). The raltitrexed-5FU-U co-crystal complex was stable at the beginning of the simulation but it shows instability starting from 22ns trajectory with fluctuation at the range (2.3Å - 4.8Å). Inspection of individual frames after 22ns trajectory revealed 5FU-U co-crystal has kept jump out from the binding site during long run simulation, thus cannot enhance the binding affinity of raltitrexed with TS (figure 3). On the other side, raltitrexed-compound 1 complex are stable with least fluctuation along the simulations at the range (1.8Å -3.8Å). In fact, this complex was more stable compared to raltitrexed-dUMP complex for longer simulation starting from 35ns trajectories. Hence, this finding indicates that compound 1 can improve the stability of raltitrexed-5FU-U co-crystal complex and it was carried forward for binding free energy calculation.

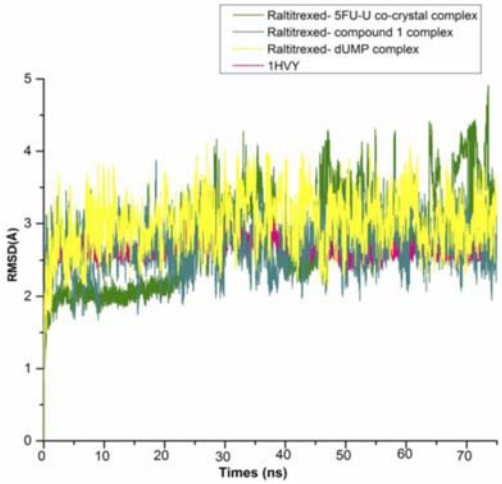

Figure 2. Molecular dynamic trajectory plot correlating root mean square deviation (Å) of the complexes within 75ns simulations.

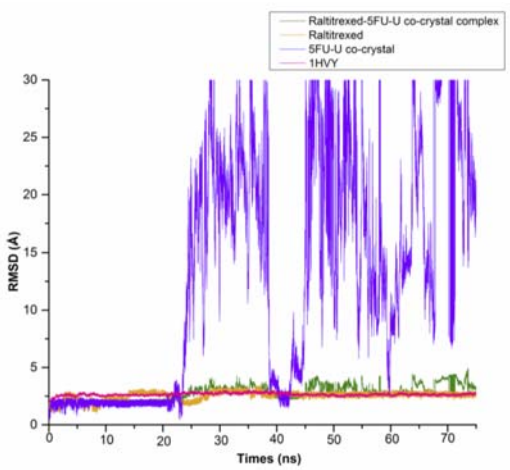

Figure 3. Individual frames of the raltitrexed-5FU-U co-crystal complex along the molecular dynamic simulations.

3.4 Binding Free Energy Calculation (MM-PBSA/GBSA)

The relative binding free energy contributions for protein-ligand complex based on MM-PBSA/GBSA were extracted from the last 5ns of simulation for each complex. The results are summarized in table 2. MM-PBSA/GBSA calculations suggested that the van der Waals (VDW) makes a major contribution to the raltitrexed-dUMP complex binding. In contrast, the contribution of binding energy for raltitrexed-compound 1 complex has mainly come from electrostatic interaction (ELE). The negative values of binding free energy of both complexes clearly demonstrate that these complexes were favourable in water. As expected, the GBSA approach indicates lower binding free energy since there was no metal in this system [29]. The more negative of the free binding energy results in the formation of stronger complexes. The compound 1 resulted in a lower total binding free energy of raltitrexed complex calculated by GBSA from -16.57 kcal/mol to -45.68 kcal/mol. Thus, this finding reveals that compound 1 has enhanced the binding affinity of raltitrexed.

Table 1. ADMET prediction of ligands.

Ligand	Raltitrexed	5-FU	Compound 1
ADMET AlogP98	2.527	-0.908	0.291
ADMET unknown AlogP98	0	0	0
ADMET PSA_2D	153.033	60.222	107.415
ADMET BBB level	4	3	3
ADMET absorption level	3	1	0
ADMET solubility	-3.9	-0.081	-1.261
ADMET solubility level	3	4	4
ADMET hepatotoxicity	1	1	1
ADMET hepatotoxicity probability	0.754	0.834	0.582
ADMET CYP2D6	0	0	0
ADMET CYP2D6 probability	0.297	0.019	0.346
ADMET PPB level	0	0	0

Table 2. MM-PBSA/GBSA calculation within last 5ns MD simulations in kcal/mol.

		Raltitrexed-dUMP complex (kcal/mol)	Raltitrexed-compound 1 complex (kcal/mol)
MM	ELE	-18.76	-88.25
	VDW	-23.66	-64.14
PBSA	PB_{SUR}	-3.75	-9.17
	PB_{CAL}	29.09	124.00
	PB_{SOL}	25.34	114.84
	PB_{ELE}	10.33	35.75
	PB_{TOT}	-17.07	-37.56
GBSA	GB_{SUR}	-2.15	-6.12
	GB_{CAL}	27.99	112.84
	GB_{SOL}	25.84	106.72
	GB_{ELE}	9.23	24.59
	GB_{TOT}	-16.57	-45.68

Note: ELE account for the electrostatic interactions. VDW denoted for Van der Waals interaction between the fragments, PB_{SUR} denotes for the non-polar contribution to solvation , PB_{CAL} is the polar contribution of solvation, PB_{SOL} is total of PB_{SUR} + $PB_{CAL,}$ PB_{ELE} account for the PB_{CAL} + ELE addition, and PB_{TOT} denotes for the total binding free energy calculated by the MM-PBSA method.

3.5 Key Interactions Residues Involving in Binding Sites of the Complex

In order to identify the key residues that involving in the binding of the complexes, per-residue free energy decomposition has been performed. Details of key residues that contribute to complex binding in the nucleotide and folate binding sites within 4**Å** from co-crystal have been interpreted as figure 4 and 5. Concerning nucleophilic catalysis is a chemical reaction that responsive to TS catalysis, catalytic Cys195A has plays a pivotal role in the nucleotide binding site [30]. The data revealed that raltitrexed-compound 1 complex have better interaction with Cys195A residue rather than raltitrexed-dUMP complex.

Insight protein-ligand interaction shows that raltitrexed-compound 1 complex have the strong interaction with His196A that mainly come from electrostatic interaction. In fact, direct interaction between the His196 imidazole and the O4 atom has been observed in the complexes of mammalian species [14]. Moreover, the binding of raltitrexed-compound 1 complex was enhanced by interactions with Arg50A, Leu192A, and Asn226A residues whilst Gly217A residue has been observed to interact with both complexes. In the folate binding site, Phe80A, Ile108A, Trp109A, Asp218A, Phe225A, Tyr258, Met311A and Ala312A were key residues that decreasing the binding energy of the complexes. The calculation also suggested that raltitrexed-compound 1 has better interaction with key residues compared to raltitrexed-dUMP complex. Overall, the most interaction for both complexes in the folate binding site is comes from electrostatic interaction rather than van der Waals forces.

Molecular dynamic simulations can explicitly analyse hydrogen bond properties

like donor-acceptor position and hydrogen bond occupancies. Hydrogen bond is one of the factors that influence the affinity between protein and ligand. The detail % occupations of hydrogen bonds in both potential binding sites within last 5 ns are represented as figure S3.

We found out that the raltitrexed-compound 1 complex exhibit intermolecular H-bond formation with several key residues rather than raltitrexed-dUMP complex. For nucleotide binding site, Asp49A and Arg215A residues play significant role in raltitrexed-dUMP complex with 99.60% and 42.92% of hydrogen bonds occupied between dUMP(OH)-(O)Asp24A and Arg215A(NH)-(O)dUMP. In contrast, strong hydrogen bonds formation of raltitrexed-compound 1 complex has been observed between Tyr135A(OH)-(O)compound 1 with 95.44% whilst moderate hydrogen bonds formed between compound 1(NH)-(N)His196A, Asn226A(NH)-(O)compound 1 and Ser191A(OH)-(O)compound 1 with 50.32%,41.12% and 33.12% of occupation, respectively. Meanwhile, in the folate binding site of raltitrexed-dUMP complex, there were moderate % hydrogen bonds occupied between raltitrexed with Lys107A, Asp218A and Glu310A. Raltitrexed-compound 1 complex exposed contradict result with tight intermolecular hydrogen bonds formed between raltitrexed(OH)-(O)Glu87A with 79.44% of hydrogen bonds occupied. The most intermolecular hydrogen bonds formed were considered as satisfied hydrogen bonds since hydrogen-acceptor distance ≤2.5Å and an angle is close to 180°.

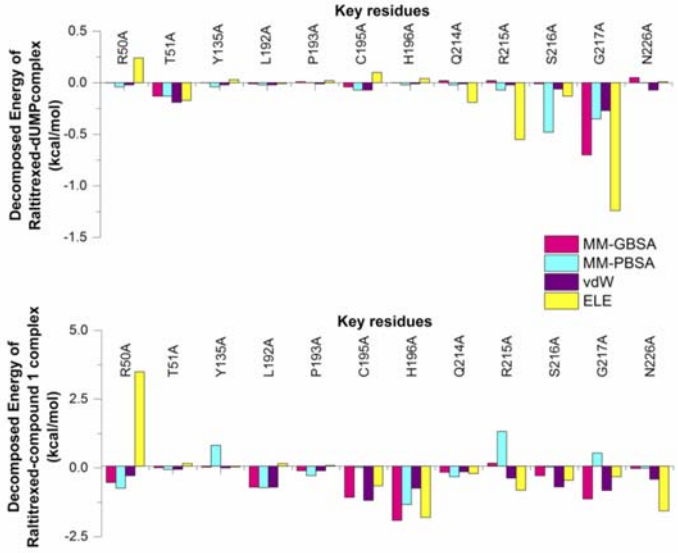

Figure 4. Key interaction residues of the nucleotide binding site within 4Å from co-crystal that contribute to the binding strength of complexes.

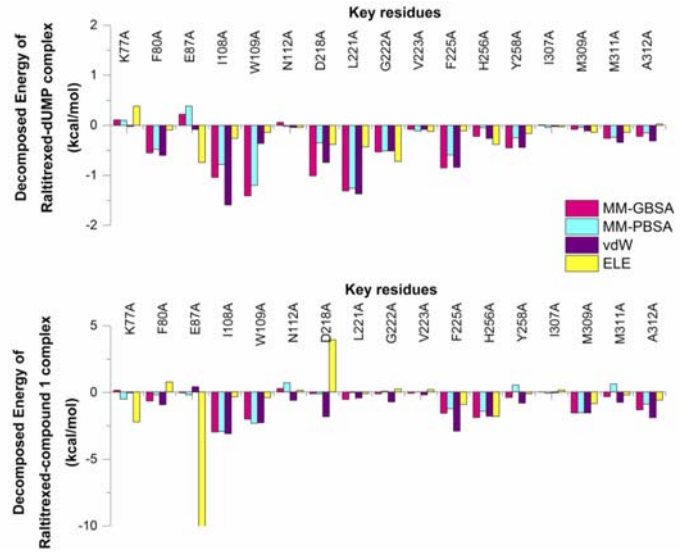

Figure 5. Key interaction residues of the folate binding site within 4Å from co-crystal that contribute to the binding strength of complexes.

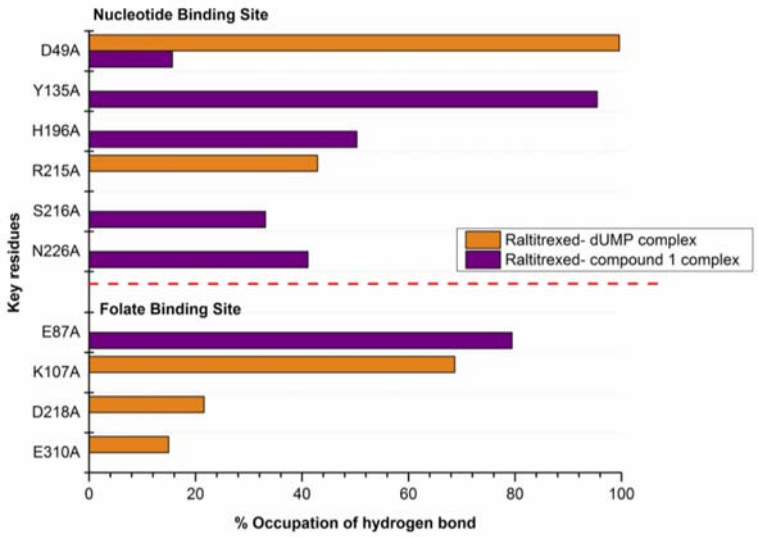

Figure S3. The percentage hydrogen bonds occupied per residue within last 5ns for both binding sites.

Due to the analysis by PLIP, the green dotted lines indicate predicted hydrogen bond of the complexes, blue dotted lines remark hydrophobic interaction, red dotted lines highlight the perpendicular π-stacking interaction and orange dotted lines shows the salt bridge formation. According to the non-covalent interaction analysis for both complexes at 75ns trajectory (figure 6), we observed that there is a conformational change of receptor upon ligand binding for raltitrexed-compound 1 complex since compound 1 is larger than dUMP.

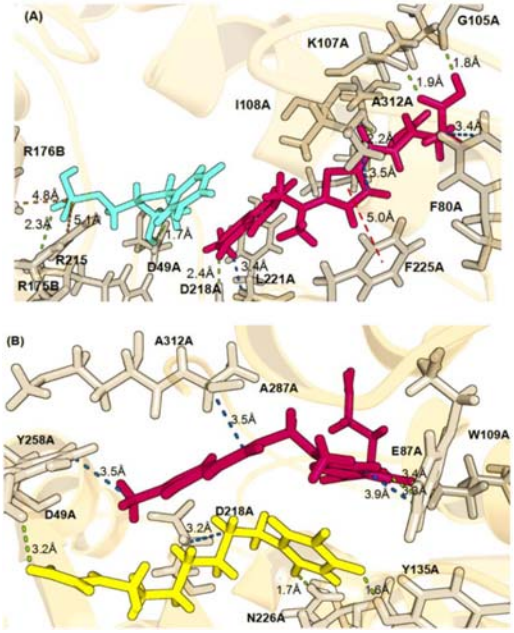

Figure 6. The non-covalent interaction for (A) raltitrexed (pink)- dUMP(blue) complex and (B) raltitrexed (pink)-compound 1(yellow) complex.

For raltitrexed-dUMP complex, dUMP shows hydrogen bonding with Asp24A, Asp174B and Arg175B at 75ns trajectory. Further, there is salt bridge formation of dUMP caused by closed interaction between Arg215A and Arg176B. Meanwhile, raltitrexed exhibits hydrogen bonds formation with Gly105A, Lys107A, Asp218A and Ala312A. Also, there were hydrophobic interactions between raltitrexed with Phe80A, Ile108A, Asp218A, and Leu196A whilst favourable perpendicular π-cation interaction with Phe225A formed caused by the interaction of cation with negative charge when the cation is near by the face of π-system. For raltitrexed-compound 1 complex, compound 1 has engaged with hydrogen bonds at Asp24A, Tyr110A, Asn226A and Arg175B residues at 75ns trajectory. Besides, hydrophobic interaction between compound 1 and Asp218A residue enhancing the interaction of the complex. On the other hands, raltitrexed displays hydrogen bonds with Glu87A and hydrophobic interactions with Val106A, Trp109A, Tyr258A and Ala287A residues.

4. Conclusion

Pharmaceutical co-crystals have emerged as a new alternative to overcome the intrinsic barrier of drug delivery. However, computational studies revealed 5FU-U co-crystal is unstable along the molecular dynamic simulation; hence it cannot enhance the binding affinity of raltitrexed in thymidylate synthase inhibition. The combination of raltitrexed with other anti-cancer drugs promising better result than monotherapy. The computational approach reveals that our modified based co-crystal, compound 1 has improved the stability of co-crystal, thus enhancing the binding affinity of raltitrexed (-45.68 kcal/mol) rather to raltitrexed alone (-16.57 kcal/mol). Decomposition energy per residue suggested that Arg50A, Leu192A, Cys195A, His196A, Asn226 and Gly217A are pivotal residues in the nucleotide binding site. The binding free energy in the folate binding site is majority come from the interaction with Phe80A, Ile108A, Trp109A, Asp218A, Phe225A, Tyr258A, Met311A and Ala312A residues. The result from ADMET indicates that compound 1 has good pharmacokinetic properties with optimum permeability and less toxicity than 5-FU. Hence, compound 1 can be further explored and developed as one of the potential anti-cancer drugs.

Acknowledgments

This research is support financially by Frontier Science Research Cluster/ UMRG Program (UMRG Project no. RP037D-17AFR).

REFERENCES

[1] Ju J., Pedersen-Lane J., Maley F. and Chu E., *Proc. Natl. Acad. Sci. USA*, 1999; **96(7)**: 3769-3774.

[2] Danenberg P.V., Leichman L., Lenz H.J., Leichman C.G. and Danenberg K.D., *Cancer Res.*, 1995; **55(7)**: 1407-1412.

[3] Wilson P.M., Danenberg P.V, Johnston P.G., Lenz H.J. and Ladner R.D., *Nature*, 2014; **11(5)**: 282-298. DOI 10.1038/nrclinonc.2014.51.

[4] Jackman A.L., Jodrell D.I., Gibson W. and Stephens T.C., ICI D1694, An Inhibitor of Thymidylate Synthase for Clinical Study; in Harkness, R.A, Elion G.B. and Zollner N., eds., *Purine and Pyrimidine Metabolism in Man VII: Part A: Chemotherapy, ATP Depletion, and Gout,* Boston, MA, 1991: 19-23.

[5] Heidelberger C., Chaudhuri N.K., Danneberg P., Mooren D., Griesbach L., Duschinsky R. and Scheiner J., *Nature*, 1957; **179(4561)**: 663-666.

[6] Van Custsem E., Cunningham D., Maroun J., Cervantes A. and Glimelius B., *Ann. Oncol.*, 2002; **13(4)**, 513-522.

[7] Nadzri N.I., Sabri N.H., Lee V.S. and Abdul Halim S.N., *J. Chem. Crystallogr.*, 2016; **46(3)**: 144-154.

[8] Becke A.D., *J. Chem. Phys.*, 1993; **98**: 5648-5652. DOI 10.1063/1.464913.

[9] Frisch M.J., Trucks G.W., Schlegel H.B., Scuseria G.E., Robb M.A., Cheeseman J.R., Scalmani G., Barone V., Mennucci B., Petersson G.A., Nakatsuji H., Caricato M., Li X., Hratchian H.P., Izmaylov A.F., Bloino J., Zheng G., Sonnenberg J.L., Hada M., Ehara M., Toyota K., Fukuda R., Hasegawa J., Ishida M., Nakajima T., Honda Y., Kitao O., Nakai H., Vreven T., Montgomery Peralta J.E., Ogliaro F., Bearpark M., Heyd J.J., Brothers E., Kudin K.N., Staroverov V.N., Kobayashi R., Normand J., Raghavachari K., Rendell A., Burant J.C., Iyengar S.S., Tomasi J., Cossi M., Rega N., Millam J.M., Klene M., Knox J.E., Cross J.B., Bakken V., Adamo C., Jaramillo J., Gomperts R., Stratmann R.E., Yazyev O., Austin A.J., Cammi R., Pomelli C., Ochterski J.W., Martin R.L., Morokuma K., Zakrzewski V.G., Voth G.A., Salvador P., Dannenberg J.J., Dapprich S., Daniels A.D., Farkas O., Foresman J.B., Ortiz J.V., Cioslowski J. and Fox D.J.,Gaussian 09, Revision A.1., Gaussian, Inc., Wallingford CT, M2009; **21**: 111.

[10] San Diego: Accelrys Software Inc.

[11] Cheng A. and Dixon S.L., *J. Comput. Aided Mol. Des.*, 2003; **17(12)**: 811-823.

[12] Dixon S.L. and Merz K.M., *J. Med. Chem. C*, 2001; **44(23)**: 3795-3809. DOI 10.1021/jm010137f.

[13] Susnow R.G. and Dixon S.L., *J. Chem. Inf. Model.*, 2003; **43(4)**: 1308-1315.

[14] Phan J., Koli S., Minor W., Dunlap R.B., Berger S.H. and Lebioda L., *Biochem. J.*, 2001; **40(7)**: 1897-1902. DOI 10.1021/bi002413i.

[15] Momany F.A. and Rone R.J., *J. Comput. Chem.*, 1992; **13**: 888-900. DOI 10.1002/jcc.540130714.

[16] Dupradeau F.Y., Pigache A., Zaffran T., Savineau C., Lelong R., Grivel N. and Cieplak P., *Phys. Chem. Chem. Phys.*, 2010; **12(28)**: 7821-7839. DOI 10.1039/C0CP00111B.

[17] Wang J., Wang W., Kollman P.A. and Case D.A., *J. Comput. Chem.*, 2004; **25**: 1157-1174. DOI 10.1002/jcc.20035.

[18] Salomon-Ferrer R., Gotz A.W., Poole D., Grand S.L. and Walker R.C., *J. Chem. Theory Comput.*, 2013; **9**: 3878-3888. DOI 10.1021/ct400314y.

[19] Case D.A., Darden T.A., Cheatham TEIII., Simmerling C.L., Wang J., Duke R.E., Luo R., Walker R.C., Zhang W., Merz K.M., Roberts B., Hayik S., Roitberg A., Seabra G., Swails J., Goetz A.W., Kolossvary I., Wong K.F., Paesani F., Vanicek J., Wolf R.M., Liu J., Wu X., Brozell S.R., Steinbrecher T., Gohlke H., Cai Q., Ye X., Wang J., Hsieh M.J., Cui G., Roe D.R., Mathews D.H., Seetin M.G., Salomon-Ferrer R., Sagui C., Babin V., Luchko T., Gusarov S., Kovalenko A. and Kollman P.A., AMBER 12. University of California, San Francisco, 2012.

[20] Dolinsky T.J., Nielsen J.E., McCammon J.A. and Baker N.A., *Nucleic Acids Res.*, 2004; **32**: W665-7. DOI 10.1093/nar/gkh381.

[21] Jorgensen W.L., *J. Phys. Chem.*, 1983; **87(26)**: 5304-5314.

[22] Essmann U., Perera L., Berkowitz M.L., Darden T., Lee H. and Pedersen L., *J. Chem. Phys.*, 1995; **103**: 8577-8592.

[23] Gotz A.W., Williamson M.J., Xu D., Poole D., Grand S.L. and Walker R.C., *J. Chem. Theory Comput.*, 2012; **8**: 1542-1555. DOI 10.1021/ct200909j.

[24] Kollman P.A., Massova I., Reyes C., Kuhn B., Huo S., Chong L., Lee M., Lee T., Duan Y., Wang W., Donini O., Cieplak P., Srinivasan J., Case D.A. and Cheatham T.E., *Acc. Chem. Res.*, 2000; **33**: 889-897.

[25] Gohlke H., Kiel C. and Case D.A., *J. Mol. Biol.*, 2003; **330(4)**: 891-913.

[26] Salentin S., Schreiber S., Haupt V.J., Adasme M.F. and Schroeder M., *Nucleic Acids Res.*, 2015; **43(W1)**: W443-W447. DOI 10.1093/nar/gkv315.

[27] Schrodinger. The PyMOL Molecular Graphics System (Version 1.6), LLC, New York, USA., 2015.

[28] Venkataramana C.H.S., Ramya Sravani K.M., Swetha Singh S. and Madhavan V., *J. Appl. Pharm. Sci.*, 2011; **1(10)**: 159-162.

[29] Hou T., Wang J., Li Y. and Wang W., *J. Chem. Inf. Model.*, 2011; **51(1)**: 69-82. DOI 10.1021/ci100275a.

[30] Santi D.V, McHenry C.S. and Sommer H., *Biochem. J.*, 1974; **13(3)**: 471-481.